
IN-CONTEXT LEARNING FOR MEDICAL IMAGE SEGMENTATION *

Eichi Takaya

AI Lab

Tohoku University Hospital

eichi.takaya.d5@tohoku.ac.jp

Shinnosuke Yamamoto

Department of Clinical Imaging

Tohoku University Graduate School of Medicine

ABSTRACT

Annotation of medical images, such as MRI and CT scans, is crucial for evaluating treatment efficacy and planning radiotherapy. However, the extensive workload of medical professionals limits their ability to annotate large image datasets, posing a bottleneck for AI applications in medical imaging. To address this, we propose In-context Cascade Segmentation (ICS), a novel method that minimizes annotation requirements while achieving high segmentation accuracy for sequential medical images. ICS builds on the UniverSeg framework, which performs few-shot segmentation using support images without additional training. By iteratively adding the inference results of each slice to the support set, ICS propagates information forward and backward through the sequence, ensuring inter-slice consistency. We evaluate the proposed method on the HVSMR dataset, which includes segmentation tasks for eight cardiac regions. Experimental results demonstrate that ICS significantly improves segmentation performance in complex anatomical regions, particularly in maintaining boundary consistency across slices, compared to baseline methods. The study also highlights the impact of the number and position of initial support slices on segmentation accuracy. ICS offers a promising solution for reducing annotation burdens while delivering robust segmentation results, paving the way for its broader adoption in clinical and research applications.

Keywords Medical Image Segmentation · In-context Learning · Semi-supervised Learning

1 Introduction

Research on AI applications in healthcare, especially automatic segmentation in medical imaging, has been actively pursued by numerous research institutions alongside advancements in deep learning technology[1][2]. Segmentation from sequential images, such as CT and MRI scans, is essential for planning surgeries and radiotherapy[3][4], as well as assessing the effectiveness of cancer treatments[5]. There is a strong demand for automating this process to reduce the burden of human effort and associated costs.

Furthermore, in the development of AI for medical image diagnosis assistance, it is often necessary to define regions of interest (ROIs) for lesion areas during the construction of training datasets. For example, ROIs are required for cropping in dimension reduction in classification tasks[6] and for generating radiomics features [7]. Moreover, it has recently been pointed out that performing lesion classification, such as distinguishing between benign and malignant conditions, on a pixel-by-pixel basis through segmentation techniques can enhance classification performance[8].

Various deep neural network architectures have been proposed, starting with U-Net [9], and in recent years, models based on Vision Transformer have become mainstream [10]. Pretrained models on large-scale datasets such as ImageNet [11] and RadImageNet [12][13], as well as foundation models capable of zero-shot inference [14][15], have also been introduced. Neural network-based approaches are becoming increasingly large-scale and are advancing in their ability to generalize across various segmentation tasks. However, challenges remain in addressing domain shifts (differences in patient populations or imaging protocols), modality shifts (variations between imaging modalities such as CT and MRI), and site shifts (differences in imaging equipment or procedures across institutions)[16][17][18]. In addition, there are limitations in the generalizability of these methods when dealing with rare diseases [19]. As a result, when attempting

**Citation:* Authors. Title. Pages.... DOI:000000/11111.

to automate specific segmentation tasks, it often becomes necessary to annotate images from scratch. Therefore, establishing a mechanism to reduce the human cost of annotating entire sequences of images from the ground up is essential.

This study aims to establish a system that minimizes the cost of annotating sequential images. To reduce the annotation load per case, we propose a sequential segmentation method based on in-context learning. Specifically, we utilize UniverSeg, a framework for few-shot segmentation proposed by Butoi et al [20]. We repeatedly input a minimal set of initial labels as support images into UniverSeg and add the outputted segmentation masks to the support set. We have named this method In-context cascade segmentation (ICS). We evaluated the proposed method using segmentation tasks for eight cardiac regions included in the HVSMR dataset [21] and discussed its effectiveness and characteristics.

The following sections are organized as follows: Section 2 provides an overview of related research on medical image segmentation, as well as discussions on in-context learning and semi-supervised learning. Section 3 clarifies the problem setting and details the proposed method. Section 4 presents the experimental details and results based on HVSMR datasets. Section 5 discusses the findings, and Section 6 concludes with future directions and challenges.

2 Related Works

2.1 Medical Image Segmentation

Before the widespread adoption of deep learning, medical image segmentation was mainly performed using traditional machine learning techniques, employing both unsupervised and supervised approaches [22]. In unsupervised approaches, clustering and region-based segmentation methods, such as K-means and watershed algorithms, were commonly used[23][24]. These methods segment regions based on statistical properties of pixels or voxels without requiring prior labeling. Supervised approaches typically involved manually designed hand-crafted features as input, using models such as support vector machines (SVMs) and random forests for pixel-wise classification [25][26]. Although these methods achieved success in certain tasks, their accuracy and generalizability were limited.

Following the study by Ciresan et al. [27], deep neural networks enabled automatic feature learning from images, facilitating segmentation. Subsequently, U-Net [9] was introduced and became a standard approach in medical image segmentation. U-Net utilizes an encoder-decoder structure and skip connections to effectively capture both local and global features, achieving high-precision segmentation. In recent years, methods based on Transformers and 3D segmentation techniques have been proposed, enabling high-accuracy segmentation for more complex structures and different modalities [28][10][29]. Additionally, large-scale medical image segmentation models, such as MedSAM [14][15] based on Segment anything model (SAM)[30][31], have emerged, allowing for high-accuracy results from minimal annotations. The UniverSeg [20] model used in our study is also a type of large-scale medical image segmentation model.

2.2 In-context Learning

In-context learning [32][33] is a concept originally introduced in large language models (LLMs), where a pre-trained model can immediately make predictions for new tasks based on examples provided within the context, without requiring additional training. In GPT-3 [34], where the term in-context learning was first used, it was shown that merely a few examples are sufficient for the model to perform tasks based on the new context. Furthermore, Oswald et al. [35] theoretically demonstrated that the mechanism enabling Transformers to perform in-context learning is similar to gradient descent.

The concept of in-context learning is also being applied to image recognition [36]. In UniverSeg [20], labeled images (support set) are provided as examples to perform segmentation on a new query image. In this study, we further develop this approach of in-context learning and apply it as "In-context Self-learning," where inference results are sequentially utilized.

2.3 Semi-supervised Learning

Semi-supervised learning is a methodology for leveraging unlabeled data when only a limited amount of labeled data is available[37]. In medical image segmentation, where labeling costs are particularly high, semi-supervised learning is frequently employed[38]. Major approaches include self-training [39], co-training [40], and graph-based methods [41], each of which has been applied to medical image segmentation. In self-training, the model re-trains itself using labels predicted from unlabeled data. Co-training involves two different classifiers complementing each other as they learn from unlabeled data. Graph-based methods represent data as a graph structure and estimate labels through label propagation.

A method closely related to our approach is 4S [42]. Based on self-training, 4S starts with a small number of consecutive labeled data slices and gradually expands the segmentation region by treating the neighboring slices as pseudo-labels. However, 4S requires re-training using these pseudo-labels each time, resulting in additional computational overhead and extended training time due to repeated parameter updates. In contrast, our proposed method does not involve explicit re-training. Instead, we leverage in-context learning to sequentially incorporate inference results into the support set, enabling more efficient segmentation while reducing computational costs.

3 Methods

3.1 Problem Definition

Given a volume dataset $V = \{\text{slice}_1, \text{slice}_2, \dots, \text{slice}_n\}$ consisting of n slices, we assume that m of these slices are available as a labeled support set. The support set is defined as follows:

$$S = \{(\text{slice}_{i_1}, \text{label}_{i_1}), (\text{slice}_{i_2}, \text{label}_{i_2}), \dots, (\text{slice}_{i_m}, \text{label}_{i_m})\},$$

where label_{i_j} represents the segmentation mask for slice i_j .

The objective of this study is to perform segmentation on the remaining $n - m$ unlabeled slices using the support set S , and to estimate the segmentation mask \hat{M}_k for each unlabeled slice slice_k . Formally, this can be expressed as follows:

Specifically, using a segmentation model f (e.g., UniverSeg), the mask \hat{M}_k for any query slice slice_k is estimated as:

$$\hat{M}_k = f(\text{slice}_k, S), \quad \text{for } k \in \{1, 2, \dots, n\} \setminus \{i_1, i_2, \dots, i_m\}.$$

3.2 UniverSeg

UniverSeg [20] is a general-purpose model designed to achieve few-shot segmentation in medical imaging. It has been trained on 53 datasets, comprising more than 22,000 examinations that include CT and MR images. Without any additional retraining, this model can quickly adapt to new segmentation tasks given only a few support sets. Structurally, UniverSeg is based on an encoder-decoder architecture and incorporates a "CrossBlock" mechanism for bidirectional feature transmission between query images and support set images. Similar to U-Net [citation], the encoder extracts features at multiple resolutions, and the decoder generates segmentation masks from these features. Pre-trained on a large-scale medical image dataset called MegaMedical, UniverSeg demonstrates the ability to adapt to various tasks and different modalities. In this study, we provide a continuous set of labeled slices as the support set and perform inference on the remaining slices (Figure 1). However, in the original UniverSeg approach, each slice is processed independently, making it difficult to ensure consistency across adjacent slices. To address this issue, we introduce a new method described next.

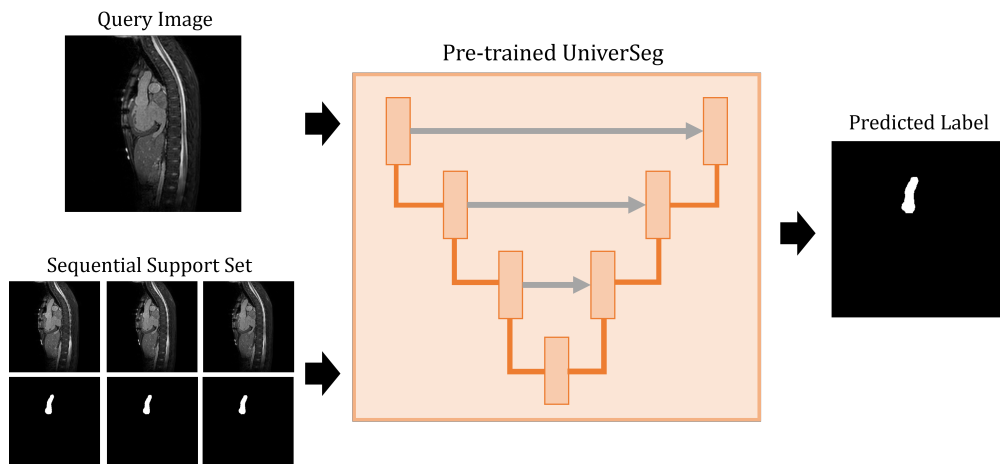


Figure 1: UniverSeg for sequential inference

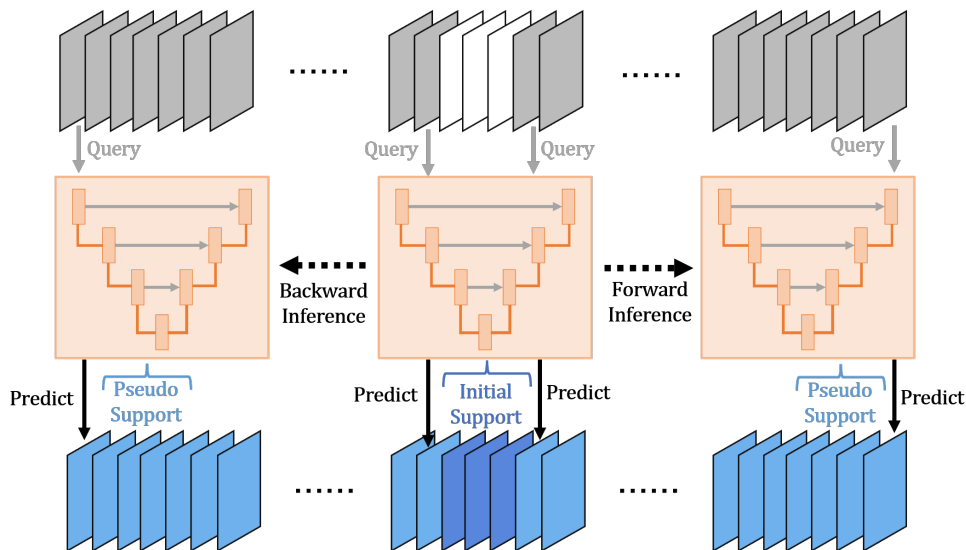


Figure 2: An overview of in-contest cascade segmentation

3.3 In-context Cascade Segmentation (ICS)

This study proposes In-context Cascade Segmentation (ICS), a method based on UniverSeg that performs sequential segmentation across an entire set of consecutive slices (Figure 2). ICS achieves consistent segmentation by using the inference results of each slice as part of the support set for the next slice, thereby propagating inference results both forward and backward through the sequence.

Although the details are described in Algorithm 1, the general flow of ICS is as follows:

1. Initialization of the Support Set
To initiate segmentation, we first set a small number of labeled slices near the center or anatomically important slices as the initial support set.
2. Bidirectional Sequential Inference
Starting from the initial support set, we apply the pre-trained UniverSeg model (trained on large-scale datasets) to perform inference in both the forward (rightward) and backward (leftward) directions across all slices. After completing the inference for each slice, we add the resulting prediction to the support set of the next slice, thereby sequentially propagating the inference results. Note that the support set is always maintained at the most recent m slices.

During this process, data augmentation is applied to the support images.

By adopting this approach, ICS improves segmentation accuracy across a continuous sequence of slices, ensuring consistency particularly at boundaries and in fine structures. Moreover, since inference is performed sequentially, the results obtained for each slice can be leveraged for subsequent slices, enabling continuous segmentation throughout the entire volume. As a result, ICS is expected to improve inter-slice consistency and accuracy compared to a direct application of UniverSeg.

4 Experiments

In this section, we conduct experiments using the HVSMR dataset [21] to verify the effectiveness and characteristics of the proposed method. We describe the dataset and experimental settings, the evaluation metrics, and the implementation details.

4.1 Dataset

HVSMR [citation] consists of 60 cardiovascular MRI (CMR) scans obtained at Boston Children’s Hospital, accompanied by segmentation masks for four cardiac chambers and four great vessels. The ground truth masks were created by

Algorithm 1 In-context Cascade Segmentation (ICS)

Require: Volume $V = \{slice_1, slice_2, \dots, slice_n\}$
Require: InitialSupportSet = $\{(img_{c_1}, label_{c_1}), \dots, (img_{c_k}, label_{c_k})\}$
Require: Model UniverSeg
Require: Maximum support set size m
Require: Augmentation function $Augment()$
Ensure: Segmented volume with label predictions for each slice in V

- 1: Initialize $ForwardSupportSet \leftarrow InitialSupportSet$
- 2: $ForwardSupportSet \leftarrow Augment(ForwardSupportSet)$
- 3: Initialize $BackwardSupportSet \leftarrow InitialSupportSet$
- 4: $BackwardSupportSet \leftarrow Augment(BackwardSupportSet)$
- 5: Initialize $ForwardPredictedLabels \leftarrow []$
- 6: Initialize $BackwardPredictedLabels \leftarrow []$
- 7: **for** $i = \max(c_1, c_2, \dots, c_k)$ **to** n **do**
- 8: $QueryImage \leftarrow slice_i$
- 9: $PredictedLabel \leftarrow UniverSeg(QueryImage, ForwardSupportSet)$
- 10: $ForwardPredictedLabels \leftarrow Append(ForwardPredictedLabels, PredictedLabel)$
- 11: $ForwardSupportSet \leftarrow Append(ForwardSupportSet, (slice_i, PredictedLabel))$
- 12: **if** $|ForwardSupportSet| > m$ **then**
- 13: Remove the oldest entries so that $|ForwardSupportSet| = m$
- 14: **end if**
- 15: $ForwardSupportSet \leftarrow Augment(ForwardSupportSet)$
- 16: **end for**
- 17: **for** $i = \min(c_1, c_2, \dots, c_k)$ **down to** 1 **do**
- 18: $QueryImage \leftarrow slice_i$
- 19: $PredictedLabel \leftarrow UniverSeg(QueryImage, BackwardSupportSet)$
- 20: $BackwardPredictedLabels \leftarrow Append(BackwardPredictedLabels, PredictedLabel)$
- 21: $BackwardSupportSet \leftarrow Append(BackwardSupportSet, (slice_i, PredictedLabel))$
- 22: **if** $|BackwardSupportSet| > m$ **then**
- 23: Remove the oldest entries so that $|BackwardSupportSet| = m$
- 24: **end if**
- 25: $BackwardSupportSet \leftarrow Augment(BackwardSupportSet)$
- 26: **end for**
- 27: **return** $ForwardPredictedLabels, BackwardPredictedLabels$

combining manual annotations with automated segmentation by a 3D-UNet, followed by human revisions. Each case includes various heart diseases and surgical histories, reflecting diverse cardiac anatomical structures across patients.

Since this study does not involve parameter tuning through training, all cases were used to evaluate the proposed method. In addition, each of the eight anatomical regions was treated as a separate dataset. As a preprocessing step, any slices that did not contain the region of interest (i.e., no annotated labels) were removed.

4.2 Experimental Settings

To examine the effectiveness and characteristics of the proposed method, we conducted the following three evaluations:

Comparison with Baseline Methods

As a baseline, we used the conventional UniverSeg. Adopting the same initial labels and augmentation settings as the proposed method, we performed inference on all slices without in-context learning.

Effect of the Number of Initial Labels

The number m of initial labeled slices in the proposed method can be chosen arbitrarily, so we investigated how this choice affects the performance. We varied m from 1 to 5.

Effect of the Position of Initial Labels

Since the position of the initial labeled slices in the proposed method can also be chosen arbitrarily, we examined how this setting influences the accuracy. We investigated this effect for all anatomical regions in one randomly selected case, setting the number of initial labeled slices m to 5.

For the above experiments, whenever there is a need to present results focusing on a specific case, we will use Patient 32, who was randomly selected.

4.3 Evaluation Metrics

We used the Dice similarity coefficient (DSC), defined by the following equation, as the performance metric for segmentation:

$$\text{DSC} = \frac{2 \cdot \text{TP}}{2 \cdot \text{TP} + \text{FP} + \text{FN}}$$

Here, TP (True Positive), FP (False Positive), TN (True Negative), and FN (False Negative) were calculated based on the predicted results and the ground truth labels at each pixel.

4.4 Implementation

All implementations of the proposed method were carried out using Python 3.10.8. For the UniverSeg model, we employed the publicly available pre-trained model from the repository provided by Butoi et al. [20]. Computations were performed on a machine equipped with an Intel(R) Core(TM) i9-10940X CPU (3.30GHz) and a Quadro RTX 8000 GPU (48GB memory).

5 Results

First, the comparison results with the baseline method are shown in Figure 3 and Table 1. From the table, ICS demonstrated significantly higher DSC ($p < 0.05$) than the baseline method in the LA, RA, AO, PA, and SVC regions. On the other hand, no significant differences were observed for the LV, RV, and IVC regions.

Figure 4 shows an example in which ICS significantly outperformed the baseline method for the PA region of Patient 32. With the baseline method, the target region was not captured adequately in response to fine structures and positional changes, resulting in discontinuous predictions and large missing areas. In contrast, ICS consistently captured the target region across the entire sequence of slices and produced stable masks in each slice. On the other hand, Figure 5 shows a case where the baseline method outperformed ICS for the LV region of the same patient. As we move toward the right side, the anatomical features change, and while the baseline method sometimes exhibited noisy predictions, there were certain slices where it delineated the region more accurately than ICS. Meanwhile, although ICS produced relatively stable masks, it tended to over-segment the target region, resulting in a higher number of false positives overall.

Table 1: Comparison of DSC statistics (mean and standard deviation) between the Baseline method and ICS for each anatomical region in the HVSMR dataset. Bold values indicate regions where ICS achieved significantly higher performance than the Baseline method ($p < 0.05$).

Region	Baseline		ICS		p-value
	Mean	Std	Mean	Std	
LV	0.5489	0.0893	0.5475	0.0770	0.8903
RV	0.4663	0.1047	0.4741	0.0933	0.3820
LA	0.3879	0.1210	0.4272	0.0925	0.0007
RA	0.5500	0.1191	0.5734	0.0791	0.0214
AO	0.4945	0.1269	0.5210	0.0679	0.0206
PA	0.3807	0.1336	0.4745	0.0974	<0.0001
SVC	0.4079	0.1805	0.4938	0.1226	<0.0001
IVC	0.4607	0.1258	0.4629	0.0871	0.8561

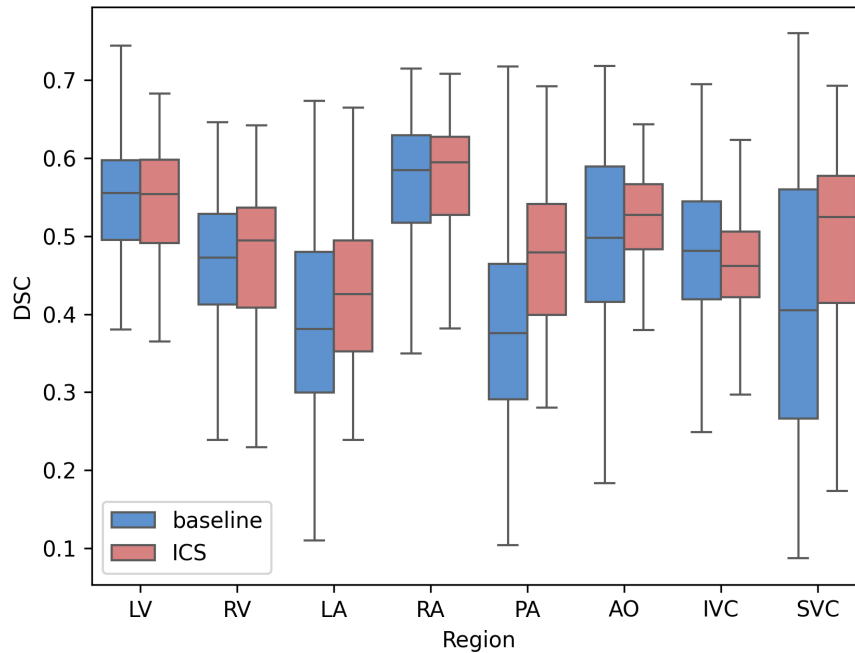


Figure 3: Box plots of the DSC for the baseline method (green) and ICS (orange) across each anatomical region. The boxes represent the interquartile range and the horizontal line within each box indicates the median.

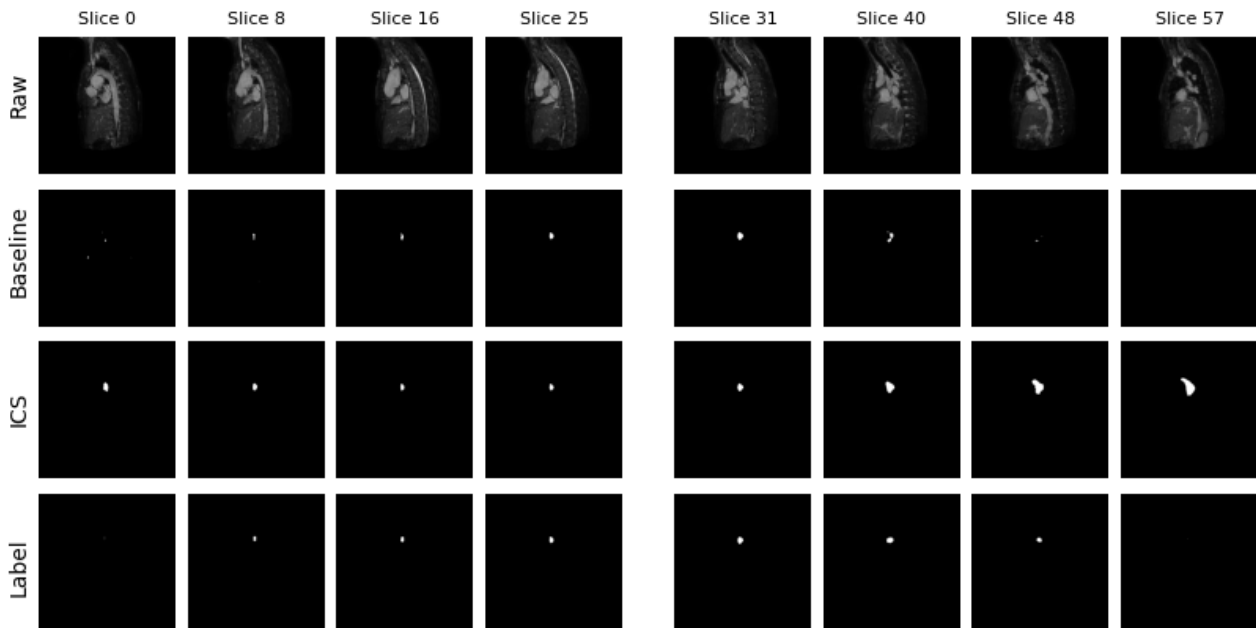


Figure 4: Segmentation results for the PA region in selected slices of a patient’s volume. From top to bottom: the raw image, the prediction by the baseline method, the prediction by ICS, and the ground truth label. Columns show different slice positions.

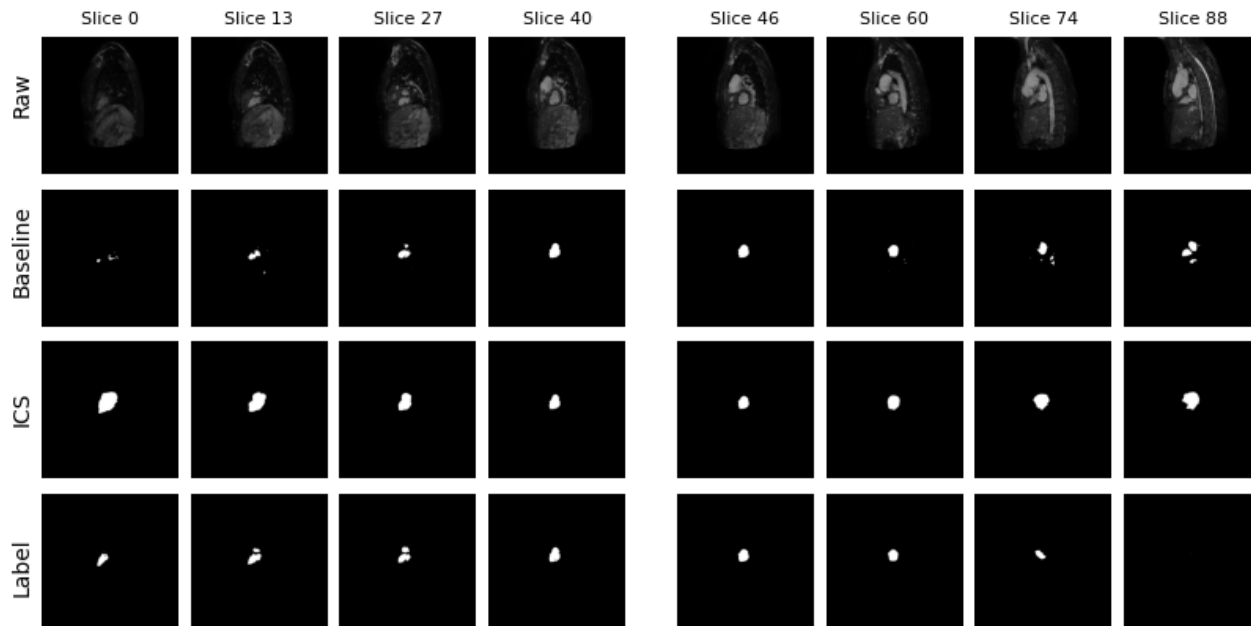


Figure 5: Segmentation results for the LV region in selected slices of a patient’s volume. From top to bottom: the raw image, the prediction by the baseline method, the prediction by ICS, and the ground truth label. Columns show different slice positions.

Figure 6 shows the slice-by-slice DSC for LV and PA in Patient 32, allowing for a quantitative confirmation of the trends observed in Figures 4 and 5. In both regions, ICS exhibits less variation between slices compared to the baseline method.

Figure 7 presents the results of experiments in which the number of initial support slices m was varied. As m increased, many regions showed a tendency for improved DSC.

Figure 8 shows the results of an experiment that exhaustively varied the positions of the initial labeled slices for each region. It was found that the initial slice settings had a substantial effect on accuracy. Moreover, while ICS outperformed the baseline method for PA and SVC regardless of the initial position, in other regions there were cases where ICS fell below the baseline depending on the initial slice placement.

6 Discussion

In this study, we conducted three comparative experiments to evaluate the effectiveness of the proposed method, In-context Cascade Segmentation (ICS). Based on the results, we provide the following discussion and subsequently address the limitations of the study.

Comparison with the Baseline Method

ICS demonstrated significantly higher DSC values compared to the baseline method (UniverSeg) in the regions of LA, RA, AO, PA, and SVC (Table 1). Particularly in PA, ICS ensured consistency across consecutive slices and accurately captured anatomically complex structures, as confirmed in Figure 4. On the other hand, no significant differences were observed in LV and IVC, with ICS exhibiting a tendency toward over-segmentation in LV, resulting in an increase in false positives (Figure 5). Overall, ICS tended to overestimate the region of interest, whereas the baseline method underestimated it. Such tendencies have also been reported in self-training-based methods [42], and this study suggests that similar behavior is present in the proposed method that replaces self-training with in-context learning. To address

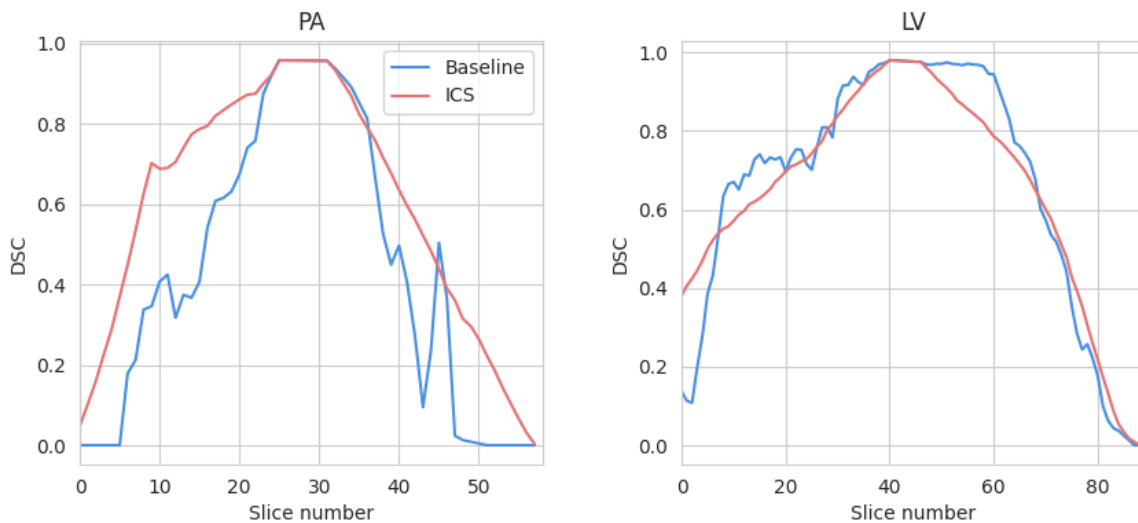


Figure 6: Line plots of the DSC for the baseline method (black) and ICS (red) across consecutive slices in the LV (left) and PA (right) regions of a selected patient. The horizontal axis indicates the slice number.

this tendency and facilitate more precise segmentation, it is necessary to introduce constraints during the support set updates, such as considering the confidence of inference results.

Effect of the Number of Initial Support Slices

In the experiment varying the number of initial support slices m , most regions showed an improvement in DSC as m increased (Figure 7). Particularly when a sufficient number of support slices were provided, ICS achieved stable segmentation results. This trend is consistent with observations from the original UniverSeg article [20]. However, in terms of computational cost, the increase in inference time and, specifically, GPU memory consumption with a higher number of support slices raises concerns. These results suggest that selecting an appropriate number of initial support slices is crucial in situations with limited computational resources. Alternatively, model distillation [43] could be employed to optimize the efficiency of the UniverSeg model itself, alongside other strategies for improving computational efficiency.

Effect of the Position of Initial Support Slices

The experiment varying the position of the initial support slices revealed that the position has a significant impact on segmentation accuracy. The DSC plot for each slice in Figure 6 shows a trend where the deviation from the ground truth increases as the distance from the initial position grows. While this suggests that the initial position should ideally be set at the center of the region of interest, it is noteworthy that this is not necessarily the case for all anatomical regions, which is an intriguing finding.

Future developments should focus on establishing methods to determine appropriate initial slices before annotation. This challenge aligns with the cold start problem in active learning [44][45], and various approaches, such as clustering-based methods, could potentially be leveraged to address it.

Limitation

The limitations of this study are outlined in two points. The first limitation is the assumption that all volumes, including the boundary slices, are labeled. In real-world data, slices that do not contain the region of interest may be present, necessitating a mechanism to appropriately stop label propagation at such slices. The second limitation is the lack of validation datasets. UniverSeg utilizes a large portion of publicly available datasets. To prevent data leakage, it was necessary to rely on the limited number of open datasets that were not used for pretraining. Consequently, this study was effectively restricted to using only the HVSMR dataset. Future work should include in-house datasets and extend the evaluation to various modalities, such as CT and ultrasound, to further validate the method.

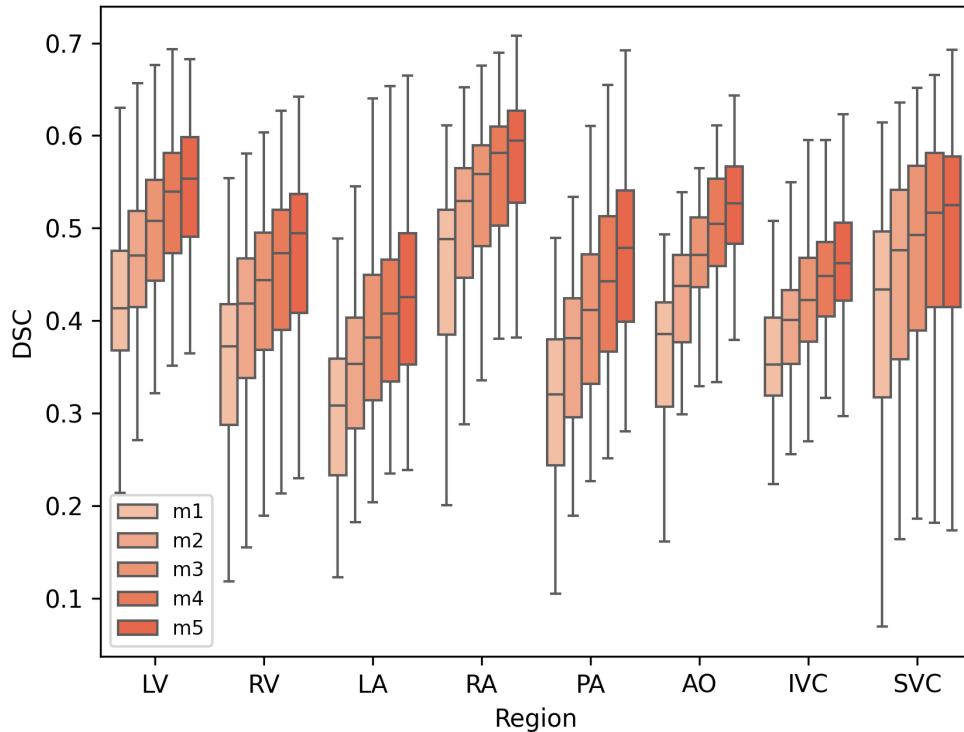


Figure 7: Box plots of the DSC for each anatomical region when varying the number of initial labeled slices m . Each color corresponds to a different m setting (from $m = 1$ to $m = 5$). The boxes represent the interquartile range, and the horizontal line within each box indicates the median.

7 Conclusion

This study proposed the In-context Cascade Segmentation (ICS) method to improve segmentation performance in sequential medical images with minimal annotations. By leveraging the UniverSeg framework, ICS sequentially updates its support set using inference results, propagating segmentation information across slices in both forward and backward directions. Through experiments on the HVSMR dataset, ICS demonstrated significant improvements over the baseline method in several anatomical regions, particularly in ensuring inter-slice consistency and accurately capturing complex structures.

The results highlighted that ICS performs well when a sufficient number of initial support slices are provided and that the position of these slices significantly impacts the segmentation accuracy. However, challenges such as over-segmentation in certain regions, the computational cost associated with a large number of support slices, and the need for effective initial slice selection were also identified. These findings suggest several avenues for future work, including the optimization of support set updates, model efficiency improvements, and the development of automated strategies for selecting optimal initial slices.

In conclusion, ICS represents a promising step toward reducing annotation burdens in medical image segmentation while maintaining high accuracy and consistency. Further validation using diverse datasets and imaging modalities will help establish its robustness and broaden its applicability in clinical and research settings.

Acknowledgments

This was supported in part by.....

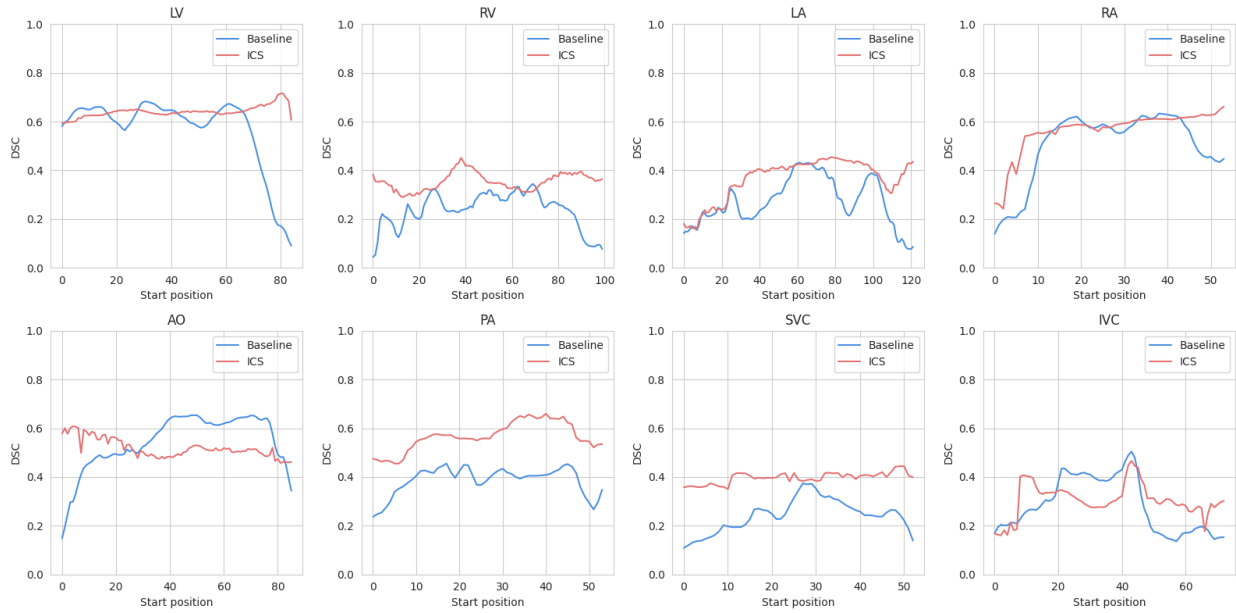


Figure 8: Line plots of the DSC for each anatomical region when varying the initial labeled slice position. The horizontal axis indicates the start position.

References

- [1] Pawan Kumar Mall, Pradeep Kumar Singh, Swapnita Srivastav, Vipul Narayan, Marcin Paprzycki, Tatiana Jaworska, and Maria Ganzha. A comprehensive review of deep neural networks for medical image processing: Recent developments and future opportunities. *Healthcare Analytics*, 4:100216, December 2023.
- [2] Reza Azad, Ehsan Khodapanah Aghdam, Amelie Rauland, Yiwei Jia, Atlas Haddadi Avval, Afshin Bozorgpour, Sanaz Karimijafarbigloo, Joseph Paul Cohen, Ehsan Adeli, and Dorit Merhof. Medical Image Segmentation Review: The Success of U-Net. *IEEE Transactions on Pattern Analysis and Machine Intelligence*, 46(12):10076–10095, December 2024.
- [3] Gauthier Dot, Thomas Schouman, Guillaume Dubois, Philippe Rouch, and Laurent Gajny. Fully automatic segmentation of craniomaxillofacial CT scans for computer-assisted orthognathic surgery planning using the nnU-Net framework. *European Radiology*, 32(6):3639–3648, June 2022.
- [4] K. Harrison, H. Pullen, C. Welsh, O. Oktay, J. Alvarez-Valle, and R. Jena. Machine Learning for Auto-Segmentation in Radiotherapy Planning. *Clinical Oncology*, 34(2):74–88, February 2022.
- [5] Yue Zhang, Chengtao Peng, Liying Peng, Yingying Xu, Lanfen Lin, Ruofeng Tong, Zhiyi Peng, Xiongwei Mao, Hongjie Hu, Yen-Wei Chen, and Jingsong Li. DeepRecS: From RECIST Diameters to Precise Liver Tumor Segmentation. *IEEE Journal of Biomedical and Health Informatics*, 26(2):614–625, February 2022.
- [6] Daiki Shimokawa, Kengo Takahashi, Ken Oba, Eichi Takaya, Takuma Usuzaki, Mizuki Kadowaki, Kurara Kawaguchi, Maki Adachi, Tomofumi Kaneno, Toshinori Fukuda, Kazuyo Yagishita, Hiroko Tsunoda, and Takuya Ueda. Deep learning model for predicting the presence of stromal invasion of breast cancer on digital breast tomosynthesis. *Radiological Physics and Technology*, 16(3):406–413, September 2023.
- [7] Takafumi Haraguchi, Yasuyuki Kobayashi, Daisuke Hirahara, Tatsuaki Kobayashi, Eichi Takaya, Mariko Takishita Nagai, Hayato Tomita, Jun Okamoto, Yoshihide Kanemaki, and Koichiro Tsugawa. Radiomics model of diffusion-weighted whole-body imaging with background signal suppression (DWIBS) for predicting axillary lymph node status in breast cancer. *Journal of X-Ray Science and Technology*, 31(3):627–640, 2023.
- [8] Sarah M Hooper, Mayee F Chen, Khaled Saab, Kush Bhatia, and Curtis Langlotz. A case for reframing automated medical image classification as segmentation.
- [9] Olaf Ronneberger, Philipp Fischer, and Thomas Brox. U-Net: Convolutional Networks for Biomedical Image Segmentation. In *Medical image computing and computer-assisted intervention, Lecture Notes in Computer Science*, volume 9351. Springer Cham, 2015.

- [10] Hu Cao, Yueyue Wang, Joy Chen, Dongsheng Jiang, Xiaopeng Zhang, Qi Tian, and Manning Wang. Swin-unet: Unet-like pure transformer for medical image segmentation. In *European conference on computer vision*, pages 205–218. Springer, 2022.
- [11] Niharika Das and Sujoy Das. Attention-UNet architectures with pretrained backbones for multi-class cardiac MR image segmentation. *Current Problems in Cardiology*, 49(1):102129, January 2024.
- [12] Xueyan Mei, Zelong Liu, Philip M. Robson, Brett Marinelli, Mingqian Huang, Amish Doshi, Adam Jacobi, Chendi Cao, Katherine E. Link, Thomas Yang, Ying Wang, Hayit Greenspan, Timothy Deyer, Zahi A. Fayad, and Yang Yang. RadImageNet: An Open Radiologic Deep Learning Research Dataset for Effective Transfer Learning. *Radiology: Artificial Intelligence*, 4(5):e210315, September 2022.
- [13] Zelong Liu, Andrew Tieu, Nikhil Patel, George Soutanidis, Louisa Deyer, Ying Wang, Sean Huver, Alexander Zhou, Yunhao Mei, Zahi A. Fayad, Timothy Deyer, and Xueyan Mei. VIS-MAE: An Efficient Self-supervised Learning Approach on Medical Image Segmentation and Classification. In Xuanang Xu, Zhiming Cui, Islem Rekik, Xi Ouyang, and Kaicong Sun, editors, *Machine Learning in Medical Imaging*, volume 15242, pages 95–107. Springer Nature Switzerland, Cham, 2025. Series Title: Lecture Notes in Computer Science.
- [14] Junde Wu, Wei Ji, Yuanpei Liu, Huazhu Fu, Min Xu, Yanwu Xu, and Yueming Jin. Medical SAM Adapter: Adapting Segment Anything Model for Medical Image Segmentation, December 2023. arXiv:2304.12620 [cs].
- [15] Jiayuan Zhu, Abdullah Hamdi, Yunli Qi, Yueming Jin, and Junde Wu. Medical SAM 2: Segment medical images as video via Segment Anything Model 2, December 2024. arXiv:2408.00874 [cs].
- [16] Cheng Ouyang, Chen Chen, Surui Li, Zeju Li, Chen Qin, Wenjia Bai, and Daniel Rueckert. Causality-Inspired Single-Source Domain Generalization for Medical Image Segmentation. *IEEE Transactions on Medical Imaging*, 42(4):1095–1106, April 2023.
- [17] Hao Guan and Mingxia Liu. Domain Adaptation for Medical Image Analysis: A Survey. *IEEE Transactions on Biomedical Engineering*, 69(3):1173–1185, March 2022.
- [18] Ling Zhang, Xiaosong Wang, Dong Yang, Thomas Sanford, Stephanie Harmon, Baris Turkbey, Bradford J. Wood, Holger Roth, Andriy Myronenko, Daguang Xu, and Ziyue Xu. Generalizing Deep Learning for Medical Image Segmentation to Unseen Domains via Deep Stacked Transformation. *IEEE Transactions on Medical Imaging*, 39(7):2531–2540, July 2020.
- [19] Navid Hasani, Faraz Farhadi, Michael A. Morris, Moozhan Nikpanah, Arman Rahmim, Yanji Xu, Anne Pariser, Michael T. Collins, Ronald M. Summers, Elizabeth Jones, Eliot Siegel, and Babak Saboury. Artificial Intelligence in Medical Imaging and its Impact on the Rare Disease Community: Threats, Challenges and Opportunities. *PET Clinics*, 17(1):13–29, January 2022.
- [20] Victor Ion Butoi, Jose Javier Gonzalez Ortiz, Tianyu Ma, Mert R. Sabuncu, John Guttag, and Adrian V. Dalca. UniverSeg: Universal Medical Image Segmentation. In *2023 IEEE/CVF International Conference on Computer Vision (ICCV)*, pages 21381–21394, Paris, France, October 2023. IEEE.
- [21] Danielle F. Pace, Hannah T. M. Contreras, Jennifer Romanowicz, Shruti Ghelani, Imon Rahaman, Yue Zhang, Patricia Gao, Mohammad Imrul Jubair, Tom Yeh, Polina Golland, Tal Geva, Sunil Ghelani, Andrew J. Powell, and Mehdi Hedjazi Moghari. HVSMR-2.0: A 3D cardiovascular MR dataset for whole-heart segmentation in congenital heart disease. *Scientific Data*, 11(1):721, July 2024.
- [22] Dzung L Pham, Chenyang Xu, and Jerry L Prince. Current methods in medical image segmentation. *Annual review of biomedical engineering*, 2(1):315–337, 2000. Publisher: Annual Reviews 4139 El Camino Way, PO Box 10139, Palo Alto, CA 94303-0139, USA.
- [23] HP Ng, SH Ong, KWC Foong, Poh-Sun Goh, and WL Nowinski. Medical image segmentation using k-means clustering and improved watershed algorithm. In *2006 IEEE southwest symposium on image analysis and interpretation*, pages 61–65. IEEE, 2006.
- [24] H.P. Ng, S.H. Ong, K.W.C. Foong, P.S. Goh, and W.L. Nowinski. Masseter segmentation using an improved watershed algorithm with unsupervised classification. *Computers in Biology and Medicine*, 38(2):171–184, February 2008.
- [25] Elisa Ricci and Renzo Perfetti. Retinal Blood Vessel Segmentation Using Line Operators and Support Vector Classification. *IEEE Transactions on Medical Imaging*, 26(10):1357–1365, October 2007.
- [26] Dwarikanath Mahapatra. Analyzing Training Information From Random Forests for Improved Image Segmentation. *IEEE Transactions on Image Processing*, 23(4):1504–1512, April 2014.
- [27] Dan C Ciresan, Luca M Gambardella, and Alessandro Giusti. Deep Neural Networks Segment Neuronal Membranes in Electron Microscopy Images. In *Proceedings of the 25th International Conference on Neural Information Processing Systems*, pages 2843–2851, 2012.

- [28] Jieneng Chen, Jieru Mei, Xianhang Li, Yongyi Lu, Qihang Yu, Qingyue Wei, Xiangde Luo, Yutong Xie, Ehsan Adeli, Yan Wang, Matthew P. Lungren, Shaoting Zhang, Lei Xing, Le Lu, Alan Yuille, and Yuyin Zhou. TransUNet: Rethinking the U-Net architecture design for medical image segmentation through the lens of transformers. *Medical Image Analysis*, 97:103280, October 2024.
- [29] Fausto Milletari, Nassir Navab, and Seyed-Ahmad Ahmadi. V-net: Fully convolutional neural networks for volumetric medical image segmentation. In *2016 fourth international conference on 3D vision (3DV)*, pages 565–571. Ieee, 2016.
- [30] Alexander Kirillov, Eric Mintun, Nikhila Ravi, Hanzi Mao, Chloe Rolland, Laura Gustafson, Tete Xiao, Spencer Whitehead, Alexander C. Berg, Wan-Yen Lo, Piotr Dollár, and Ross Girshick. Segment Anything. In *2023 IEEE/CVF International Conference on Computer Vision (ICCV)*, pages 3992–4003, Paris, France, October 2023. IEEE.
- [31] Nikhila Ravi, Valentin Gabeur, Yuan-Ting Hu, Ronghang Hu, Chaitanya Ryali, Tengyu Ma, Haitham Khedr, Roman Rädle, Chloe Rolland, Laura Gustafson, Eric Mintun, Junting Pan, Vasudev Alwala, Nicolas Carion, Chao-Yuan Wu, Ross Girshick, Piotr Dollár, and Christoph Feichtenhofer. SAM 2: Segment Anything in Images and Videos.
- [32] Qingxiu Dong, Lei Li, Damai Dai, Ce Zheng, Jingyuan Ma, Rui Li, Heming Xia, Jingjing Xu, Zhiyong Wu, Tianyu Liu, Baobao Chang, Xu Sun, Lei Li, and Zhifang Sui. A Survey on In-context Learning, October 2024. arXiv:2301.00234 [cs].
- [33] Sewon Min, Xinxu Lyu, Ari Holtzman, Mikel Artetxe, Mike Lewis, Hannaneh Hajishirzi, and Luke Zettlemoyer. Rethinking the Role of Demonstrations: What Makes In-Context Learning Work?, October 2022. arXiv:2202.12837 [cs].
- [34] Tom Brown, Benjamin Mann, Nick Ryder, Melanie Subbiah, Jared D Kaplan, Prafulla Dhariwal, Arvind Neelakantan, Pranav Shyam, Girish Sastry, Amanda Askell, and others. Language models are few-shot learners. *Advances in neural information processing systems*, 33:1877–1901, 2020.
- [35] Johannes von Oswald, Eyvind Niklasson, Ettore Randazzo, João Sacramento, Alexander Mordvintsev, Andrey Zhmoginov, and Max Vladymyrov. Transformers learn in-context by gradient descent, May 2023. arXiv:2212.07677 [cs].
- [36] Yuanhan Zhang, Kaiyang Zhou, and Ziwei Liu. What makes good examples for visual in-context learning? *Advances in Neural Information Processing Systems*, 36:17773–17794, 2023.
- [37] Jesper E. van Engelen and Holger H. Hoos. A survey on semi-supervised learning. *Machine Learning*, 109(2):373–440, February 2020.
- [38] Rushi Jiao, Yichi Zhang, Le Ding, Bingsen Xue, Jicong Zhang, Rong Cai, and Cheng Jin. Learning with limited annotations: A survey on deep semi-supervised learning for medical image segmentation. *Computers in Biology and Medicine*, 169:107840, February 2024.
- [39] Krishna Chaitanya, Ertunc Erdil, Neerav Karani, and Ender Konukoglu. Local contrastive loss with pseudo-label based self-training for semi-supervised medical image segmentation. *Medical Image Analysis*, 87:102792, July 2023.
- [40] Yingda Xia, Dong Yang, Zhiding Yu, Fengze Liu, Jinzheng Cai, Lequan Yu, Zhuotun Zhu, Daguang Xu, Alan Yuille, and Holger Roth. Uncertainty-aware multi-view co-training for semi-supervised medical image segmentation and domain adaptation. *Medical Image Analysis*, 65:101766, October 2020.
- [41] Mengzhu Wang, Jiao Li, Houcheng Su, Nan Yin, Liang Yang, and Shen Li. GraphCL: Graph-based Clustering for Semi-Supervised Medical Image Segmentation, November 2024. arXiv:2411.13147 [cs].
- [42] Eichi Takaya, Yusuke Takeichi, Mamiko Ozaki, and Satoshi Kurihara. Sequential semi-supervised segmentation for serial electron microscopy image with small number of labels. *Journal of Neuroscience Methods*, 351:109066, March 2021.
- [43] Jianping Gou, Baosheng Yu, Stephen J. Maybank, and Dacheng Tao. Knowledge Distillation: A Survey. *International Journal of Computer Vision*, 129(6):1789–1819, June 2021.
- [44] Qiuye Jin, Mingzhi Yuan, Shiman Li, Haoran Wang, Manning Wang, and Zhijian Song. Cold-start active learning for image classification. *Information Sciences*, 616:16–36, November 2022.
- [45] Salome Kazeminia, Miroslav Březík, Sayedali Shetab Boushehri, and Carsten Marr. A Data-Driven Solution for The Cold Start Problem in Biomedical Image Classification. In *2024 IEEE International Symposium on Biomedical Imaging (ISBI)*, pages 1–5, Athens, Greece, May 2024. IEEE.